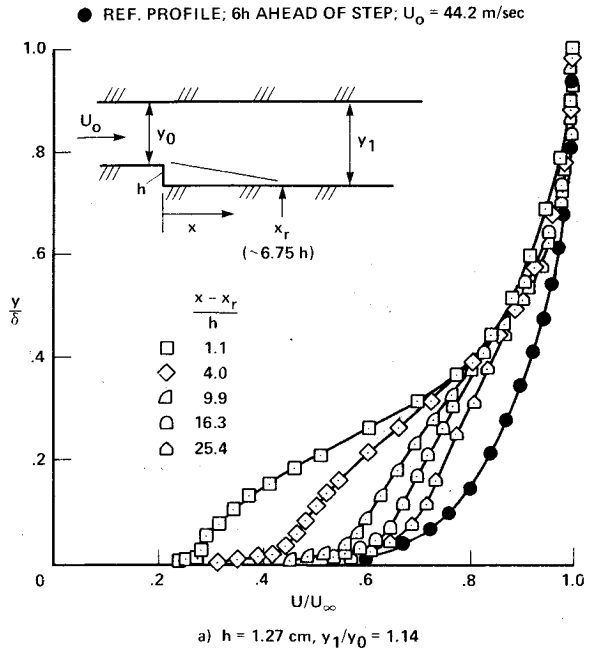

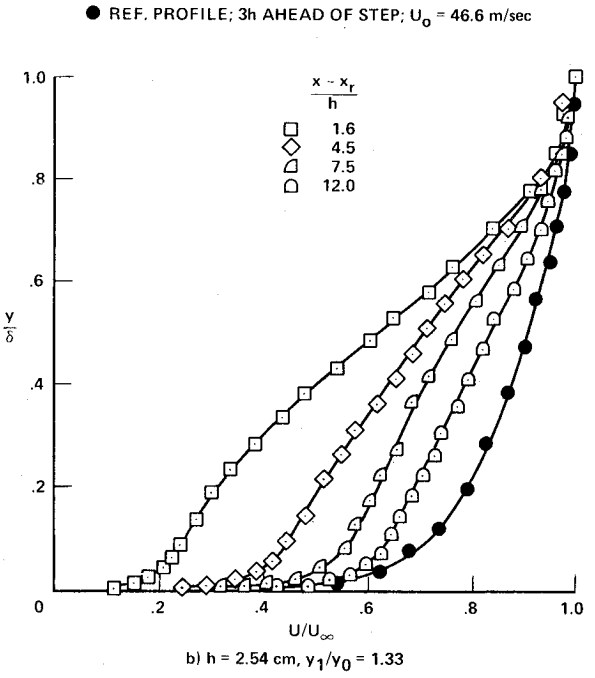

Fig. 2 Velocity profiles downstream of reattachment for two values of y_1/y_0: a) $h = 1.27$ cm, $y_1/y_0 = 1.14$; b) $h = 2.54$ cm, $y_1/y_0 = 1.33$.

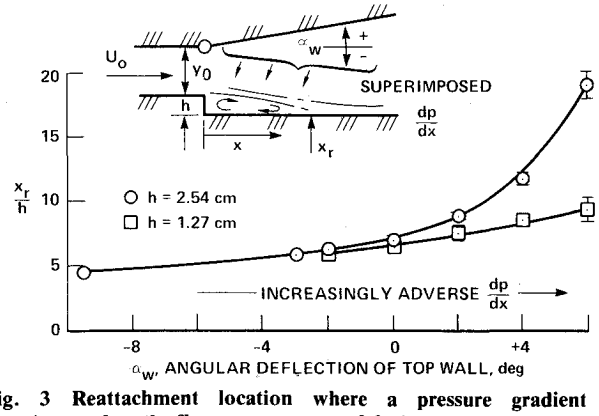

Fig. 3 Reattachment location where a pressure gradient is superimposed on the flow over a rearward-facing step; $U_0 \sim 45$ m/s.

imposed adverse pressure gradient was reduced by a superimposed favorable gradient. This caused the reattachment region to move closer to the step. When an adverse gradient was superimposed on the adverse gradient due to the step expansion, reattachment moved far downstream.

Conclusions

These data show a large influence of adverse pressure gradient on the reattaching flow over a rearward-facing step that has not been reported previously. Further, the many previous experiments for fully developed, turbulent flow in parallel-walled channels have shown a range of reattachment location that has not been explained by differences in initial flow conditions. Although these initial flow conditions might contribute to the observed variation of reattachment location, it appears that the pressure gradient effect can explain most of that variation.

References

[1] Badri Narayanan, M.A., Khadgi, Y.N., and Viswanath, P. R., "Similarities in Pressure Distribution in Separated Flow Behind Backward-Facing Steps," *Aeronautical Quarterly*, Vol. 25, Pt. 4, Nov. 1974, pp. 305-312.

[2] Kim, J., Kline, S.J., and Johnston, J.P., "Investigation of Separation and Reattachment of a Turbulent Shear Layer: Flow Over a Backward-Facing Step," MD-37, Thermoscience Division, Dept. of Mech. Eng., Stanford Univ., April 1978.

[3] Eaton, J.K., Johnston, J.P., and Jeans, A.H., "Measurements in a Reattaching Turbulent Shear Layer," Rept. IL-5, presented at the Second Symposium on Turbulent Shear Flows, Imperial College, London, July 2-4, 1979.

NH

J80-063

Use of Metallic Analog Materials in Low-Gravity Solidification Experiments

30020
80002

John M. Papazian*
Grumman Aerospace Corporation, Bethpage, N.Y.

As part of the NASA space processing effort, several solidification experiments have been performed which used aqueous ammonium chloride solutions (NH_4Cl:H_2O) as a model material.[1,2] The transparency and ease of handling of this material make it attractive from an experimenter's point of view, and the dendritic nature of its solid-liquid interface provides a good analog for metallic systems.[3] Since convective effects can be very significant in solidification experiments and since differences exist between the thermophysical properties of aqueous and metallic liquids, some care must be taken in translating experimental conclusions from one class of materials to the other. Several authors have considered this problem,[4,5] and a convection analysis of one of the low-gravity experiments has been published.[6] This analysis concluded that, for the particular experimental geometry under consideration, aqueous and metallic convective velocities expected in the low-gravity rocket experiment are of insignificant magnitudes and that crystallization phenomena observed in such experiments using

Received June 27, 1979; revision received Aug. 17, 1979.

Index categories: Space Processing; Materials, Properties of.

*Staff Scientist, Research Dept.

aqueous analogs may be indicative of metallic behavior.[6] This conclusion is correct insofar as convective velocities are concerned, but it ignores the large differences in thermal properties between aqueous and metallic liquids. It is the purpose of this Note to show that these differences can have a significant effect on the comparative solidification behavior and to illustrate this conclusion with results from two SPAR experiments.

The results of one of the SPAR V rocket experiments showed that the reduced gravity environment significantly modified the thermal conditions in the liquid portion of the NH_4Cl:H_2O samples.[2] It was found that, in low gravity, the center of the sample cooled at a much slower rate than in otherwise identical one-gravity experiments. These modified thermal conditions resulted in a completely columnar microstructure of the solidified sample whereas, in one gravity, the microstructure was up to 75% equiaxed. The change in thermal conditions was presumed to be due to the elimination of natural convection as a heat transport mechanism. Simple calculations can be made which support this view, as follows.

The proportion of heat transported by convection can be expressed in terms of a generalized Nusselt number[5]

$$Nu = (Q_{cond} + Q_{conv})/Q_{cond} \quad (1)$$

where Q_{cond} and Q_{conv} are the amounts of heat transported by conduction and convection, respectively. In Fig. 4 of Ref. 5, Cole presents a correlation between this Nusselt number and the Rayleigh number, Ra, for heat transfer in horizontal cylinders. Using this correlation as a rough guide, we can estimate the Nusselt number for the conditions that existed at the beginning of the experiment. Values of the Rayleigh number for the solidification chamber were first calculated from the expression

$$Ra = g\rho\beta\Delta T H^3/\mu\alpha \quad (2)$$

where g is the acceleration of gravity, ρ the liquid density, β the thermal coefficient of volume expansion, ΔT the temperature difference, H the height, μ the viscosity, and α the thermal diffusivity. Typical values of the experimental parameters were taken as $H = 15$mm and $\Delta T = 45$ K. The Rayleigh numbers and the corresponding Nusselt numbers so obtained are given in Table 1 for $g = g_o$ (9.8 m/s^2), and for $g = 10^{-4}\ g_o$. The Rayleigh number is directly proportional to g; thus values for $g = 10^{-4}\ g_o$ are not listed. Also shown in the table are values of these numbers for four other materials: succinonitrile ($C_4H_4N_2$), iron, lead, and copper. Succinonitrile is an organic liquid which has been used as a metal model material[3] and iron, lead, and copper were chosen as three typical metals. Finally, the Prandtl numbers for each liquid are listed in Table 1. (The Prandtl number is the ratio of momentum diffusivity to thermal diffusivity.) It can be seen that for water or succinonitrile, in the sample configuration of this experiment, the Nusselt number is reduced by almost a factor of 10 when going from normal gravity to $10^{-4} g_o$. Since Q_{cond} is the same in both one gravity and low gravity, this result is consistent with the observations of significantly reduced heat transport in the low-gravity experiment using NH_4Cl:H_2O. This behavior is expected to be typical of high Prandtl number liquids.

Table 1 Dimensionless numbers for five materials

	H_2O	$C_4H_4N_2$	Fe	Pb	Cu
$Ra(g=g_o)$	3×10^6	4×10^6	2×10^4	3×10^4	3×10^3
$Nu(g=g_o)$	25	25	3	3	1.3
$Nu(g=10^{-4}g_o)$	3	3	1	1	1
Pr	7	23	0.07	0.003	0.003

Metals, which typically have much lower Prandtl numbers, behave in a qualitatively similar manner, i.e., their Nusselt numbers are reduced, but the differences between one gravity and reduced gravity are much less pronounced. The Nusselt numbers in iron and lead would drop by a factor of 3; but in copper, the heat transport would be practically unchanged by the elimination of convection. Thus, an experiment similar to that in SPAR V, but using a metal, copper in particular, as the sample material, might yield significantly different results. No significant change in the thermal conditions in the sample would be observed when going from one gravity to low gravity and, hence, no concomittant change in the solidification microstructure would be expected.

The substantial reduction in heat transport in high Prandtl number fluids observed in the low-gravity experiment and illustrated by the preceding calculation suggests an explanation for the hitherto puzzling results of one of the SPAR I experiments.[7] In that experiment, cyclohexanol, contained in a standard quartz spectrophotometer cell,† was solidified by cooling the bottom of the cell. Cyclohexanol is an organic plastic crystal compound which, like succinonitrile, is used to model metallic solidification.[3] In the SPAR I experiment, solidification in one gravity always proceeded in an aligned columnar manner; but in low gravity, repeated nucleation ahead of the interface was observed and an equiaxed structure resulted.[7] The Rayleigh number for that geometry was roughly 10^5 in one gravity; thus the Nusselt number changed from about 11 in one gravity to 1.5 in low gravity. This reduction of thermal transport in the liquid in low gravity resulted in a situation in which the thermal transport in the quartz wall of the cell ($K = 1.3$ W/mK) was greater than that of the cyclohexanol, liquid or solid ($K = 0.1$ W/mK). Thus, the wall became a preferred path for conduction of heat out of the solution, cooling the liquid near the wall ahead of the solid-liquid interface to below its liquidus and causing nucleation. In this case, therefore, the reduced heat transport in low gravity caused the aligned, columnar, one gravity structure to change to an equiaxed structure in low gravity. This is exactly the opposite of the SPAR V result discussed earlier; but both changes in microstructure appear to have been caused by the gravity related reduction in thermal transport in the liquid. A comparable, equiaxed, result[8] appears to have been obtained in the SPAR V flight of experiment 74-21 in which an NH_4Cl:H_2O solution was solidified in a quartz cell that was very similar to that of the SPAR I experiment described in Ref. 7.

The contrasting results emphasize the importance attached to detailed consideration of the experimental conditions, reinforce the conclusion that modification of the thermal conditions in the liquid can be the most important effect of reduced gravity on experiments of this type, and further illustrate the need to consider the differences between the properties of the materials in question before extrapolating low-gravity results from one system to another.

References

[1] Johnston, M. H. and Griner, C. S., "The Direct Observation of Solidification as a Function of Gravity Level", *Metallurgical Transactions A*, Vol. 8A, Jan. 1977, pp. 77–82.

[2] Papazian, J. M. and Kattamis, T. Z., "The Effect of Reduced Gravity on the Solidification Microstructures of NH_4Cl-H_2O Alloys," *Metallurgical Transactions*, in press, 1980.

[3] Jackson, K. A. and Hunt, J. D., "Transparent Compounds that Freeze Like Metals," *Acta Metallurgica*, Vol. 13, 1965, pp. 1212–1215.

[4] Cole, G. S. and Bolling, G. F., "Visual Observations of Crystallization from Aqueous Solution Under Enforced Fluid Motion," *Transactions TMS-AIME*, Vol. 239, Nov. 1967, pp. 1860–1861.

†The overall dimensions of the cell were $10\times10\times45$ mm and the walls were 1 mm thick optically flat quartz.

[5]Cole, G. S., "Transport Processes and Fluid Flow in Solidification," *Solidification,* American Society for Metals, 1971, pp. 201-274.

[6]Grodzka, P. G., Johnston, M. H., and Griner, C. S., "Convection Analysis of the Dendrite Remelting Rocket Experiment," *AIAA Journal,* Vol. 16, May 1978, pp. 417-418.

[7]Papazian, J. M. and Kattamis, T. Z., "Contained Polycrystalline Solidification in Low Gravity, Experiment 74-37," *Space Processing Applications Rocket Project SPAR I Final Report,* NASA TMX-3458, Dec. 1976, pp. VIII-1 - VIII-21.

[8]Johnston, M. H., private communication, March 1979.

J80-064

On the Fundamental Solution for a Cascade

T.F. Balsa*
General Electric Corporate Research and Development
Schenectady, N.Y.

IN the theories of compressor blade flutter, of noise generation by or transmission through fans, and of lift fluctuations on a cascade due to inlet disturbances, one is interested in a certain fundamental solution, say p, to the wave equation. This fundamental solution satisfies

$$\left(\frac{\partial}{\partial t}+U_\infty\frac{\partial}{\partial x}\right)^2 p-c_\infty^2\left(\frac{\partial^2 p}{\partial x^2}+\frac{\partial^2 p}{\partial y^2}\right)$$

$$=\sum_{n=-\infty}^{\infty} e^{i\omega t}e^{in\sigma}\delta(x-sn\cos\lambda)\delta(y-sn\sin\lambda) \qquad (1)$$

where $U_\infty=\text{const}$, $c_\infty=\text{const}$ are the undisturbed flow velocity and speed of sound in the medium, and t and (x,y) denote time and Cartesian space coordinates, respectively (see Fig. 1). The right-hand side of Eq. (1) represents an infinite array of pressure sources placed along the line $y-x\tan\lambda=0$; these sources are separated by a constant distance s and are harmonically oscillating at a circular frequency ω. The phase difference between adjacent sources is σ. [Note: $i=(-1)^{1/2}$ and $\delta=\delta(\xi)$ denotes the delta function.]

The long time solution ($t\to\infty$) to Eq. (1) is expressible as $p=P\exp(i\omega t)$, where P consists of a poorly converging infinite series of Bessel functions. Kaji and Okazaki[1] have shown how to render this infinite series rapidly convergent in the subsonic case (i.e., $U_\infty/c_\infty=M<1$) by a clever and complex application of the Poisson summation formula.

The purpose of this Note is twofold: first to show that the essential results of Kaji and Okazaki may be obtained by a simpler alternate route, and, second, to point out that these results are valid not only in the strictly subsonic case ($M<1$) but also in the subsonic leading edge case, $M\sin\lambda<1$ but $M>1$.

To do this, Eq. (1) is solved with *initial* conditions $p=\partial p/\partial t=0$ at $t=0$. While this procedure apparently implies added complexity, this is not the case because the required sum is evaluated readily. First consider the solution , p_n, for a single source, say the nth one. It is known[2] that

$$p_n=\frac{e^{i\omega t}e^{in\sigma}}{2\pi c_\infty}\int_0^t e^{-i\omega T}\frac{H(\zeta)}{\zeta^{1/2}}\,dT \qquad (2a)$$

Received April 19, 1979; revision received Aug. 21, 1979.

Index categories: Airbreathing Propulsion; Nonsteady Aerodynamics; Aeroelasticity and Hydroelasticity.

*Mechanical Engineer. Member AIAA.

where $\zeta=c_\infty^2T^2-(x-sn\cos\lambda-U_\infty T)^2-(y-sn\sin\lambda)^2$ and by superposition

$$p=\sum_{n=-\infty}^{\infty}p_n \qquad (2b)$$

Here $H(\zeta)$ denotes the Heaviside function such that $H=1$ for $\zeta>0$ and $H=0$ for $\zeta<0$.

If now the order of the integration and summation is interchanged in Eq. (2b) after Eq. (2a) is substituted for p_n, then a *finite* sum is first needed evaluation. It is known[3] that

$$\sum_{n=-\infty}^{\infty}\frac{e^{in\sigma}H(\zeta)}{\zeta^{1/2}}=\frac{\pi}{s}e^{-i\alpha\xi/s}\sum_{n=-\infty}^{\infty}e^{2\pi in\xi/s}J_0\{\eta^{1/2}(2\pi n-\sigma)/s\} \qquad (3)$$

where

$$\xi=-(x-U_\infty T)\cos\lambda-y\sin\lambda$$

$$\eta=c_\infty^2T^2-[(x-U_\infty T)\sin\lambda-y\cos\lambda]^2$$

and J_0 is a Bessel function. It is emphasized that the sum on the left-hand side of Eq. (3) is finite because of the H function. Finally, as $t\to\infty$, an integral (actually a Fourier transform) with respect to T is left. This is again standard,[4] so the final result is

$$p=\frac{\exp[i\omega(t-\tilde{y}M\sin\lambda/c_\infty\beta)]}{2c_\infty^2}\Big[\sum_n\exp$$

$$[i(2\pi n-\sigma)(\tilde{y}M^2\sin\lambda\cos\lambda/\beta-\tilde{x})/s]\times\frac{\exp[-|\tilde{y}/s\beta|\Gamma^{1/2}]}{\Gamma^{1/2}}$$

$$+\sum_n\exp[i(2\pi n-\sigma)(\tilde{y}M^2\sin\lambda\cos\lambda/\beta-\tilde{x})/s]$$

$$\times i\{\operatorname{sgn}[(2\pi n-\sigma)M\cos\lambda-\omega s/c_\infty]\cos[|\tilde{y}|(-\Gamma)^{1/2}/s\beta]$$

$$+i\sin[|\tilde{y}|(-\Gamma)^{1/2}/s\beta]\}/(-\Gamma)^{1/2}\Big] \qquad (4a)$$

where $\tilde{x}$ and $\tilde{y}$ are the rotated coordinates $\tilde{x}=x\cos\lambda+y\sin\lambda$, $\tilde{y}=-x\sin\lambda+y\cos\lambda$, and $\beta=1-M^2\sin^2\lambda$. Here Γ is the *propagation parameter*

$$\Gamma=(2\pi n-\sigma)^2(1-M^2\sin^2\lambda)-[(2\pi n-\sigma)M\cos\lambda-\omega s/c_\infty]^2 \qquad (4b)$$

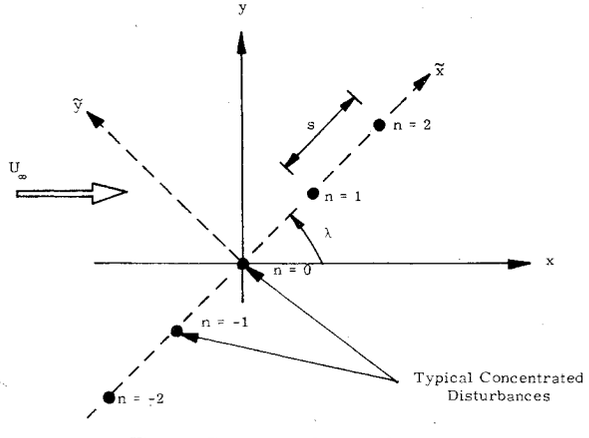

Fig. 1 Geometry of the problem.